

## **ATP Analog Enhances the Actions of a HSP90 Inhibitor in Multiple Myeloma Cells**

Fabiola Cervantes-Gomez, Ramadevi Nimmanapalli, and Varsha Gandhi.

Departments of Experimental Therapeutics (F.G. and V.G.) and Leukemia (V.G.), The University of Texas MD Anderson Cancer Center, Houston, Texas; Graduate School of Biomedical Sciences, The University of Texas Health Science Center, Houston, Texas; and Department of Pathobiology, College of Veterinary Medicine, Nursing, and Allied Health, Tuskegee University, Tuskegee, Alabama (R.N.).

**Running Title:** 8-Cl-Ado enhances the actions of 17-AAG in myeloma cells

**Requests for Reprints:** Varsha Gandhi, Department of Experimental Therapeutics, Unit 71,  
The University of Texas MD Anderson Cancer Center, 1515 Holcombe Blvd., Houston, TX  
77030. Phone: 713-792-2989; Fax: 713-794-4316; E-mail: [vgandhi@mdanderson.org](mailto:vgandhi@mdanderson.org).

**Pages:** 27.

**Tables:** 1.

**Figures:** 6.

**References:** 40.

**Abstract:** 181 words.

**Introduction:** 735 words.

**Discussion:** 1420 words.

**Abbreviations:** 17-*N*-Allylamino-17-demethoxygeldanamycin (17-AAG), 8-Chloro-Adenosine (8-Cl-Ado), heat shock factor (HSF-1), heat shock protein 90 (HSP90), HSP90/HSP70 organizing protein (HOP).

**Recommended section:** Chemotherapy, Antibiotics, and Gene Therapy.

**Abstract** (word count 181)

Heat shock protein 90 (HSP90) regulates client oncoprotein maturation. HSP90's chaperone function is blocked by 17-*N*-Allylamino-17-demethoxygeldanamycin (17-AAG), although it results in transcription and translation of antiapoptotic HSP proteins. Using three myeloma cell lines we tested if inhibition of transcription/translation of HSP or client proteins will enhance 17-AAG-mediated cytotoxicity. 8-Chloro-Adenosine (8-Cl-Ado), currently in clinical trials, inhibits bioenergy production, mRNA transcription, and protein translation and was combined with 17-AAG. 17-AAG treatment resulted in HSP transcript and protein level elevation. In the combination, 8-Cl-Ado did not abrogate HSP mRNA and protein induction. HSP90 requires ATP to stabilize client proteins, hence, expression of STAT3, Raf-1, and Akt were analyzed. 17-AAG alone resulted in <10% change in STAT3, Raf-1, and Akt protein levels, while no change was observed for 4E-BP1. In contrast, the combination treatment resulted in >50% decrease of client protein levels and marked hypophosphorylation of 4E-BP1. 8-Cl-Ado alone resulted in <30% decrease of client proteins and 4E-BP1 hypophosphorylation. 8-Cl-Ado combined with 17-AAG resulted in more than additive cytotoxicity. In conclusion, 8-Cl-Ado that targets transcription, translation and cellular bioenergy, enhanced 17-AAG-mediated cytotoxicity in myeloma cells.

## Introduction

The HSP family is a group of highly conserved constitutive and stress-inducible related proteins that act as molecular chaperones assisting in protein folding and stabilization (Hartl and Hayer-Hartl, 2002). Cytosolic HSP90 $\alpha/\beta$  is the most abundant chaperone in the cell. An increase in the levels of this chaperone is further observed when the cell is subjected to physiological stress (including hypoxia, heat, heavy metals, and small molecules like 17-AAG) (Whitesell and Lindquist, 2005). HSP90 is essential in the stabilization and functional conformation of stress-denatured client oncoproteins. Hence, inhibition of the re-folding activity of HSP90 would result in the simultaneous downregulation of signaling cascades (Sharp and Workman, 2006; Biamonte et al., 2010). HSP90 chaperone activity is an ATP-dependent process (Prodromou et al., 1997). A denatured client protein is recognized by cochaperones HSP70 and HSP40 priming it in preparation for loading onto HSP90 (Pratt and Toft, 2003), which is facilitated by the cochaperone HSP90/HSP70 organizing protein (HOP) (Smith et al., 1993; Onuoha et al., 2008). Once the unfolded client interacts with HSP90, ATP binds to the ATP binding pocket in HSP90 and subsequent cochaperones bind to the client•HSP90 complex, facilitating its stabilization. A change in HSP90 conformation triggers ATP hydrolysis catalyzing the maturation and functional stability of the client protein (Whitesell and Lindquist, 2005; Biamonte et al., 2010).

Given the importance of the HSP90 chaperone cycle in the stability of oncoproteins, several inhibitors of HSP90 have been identified including geldanamycin and its analog derivative 17-*N*-Allylamino-17-demethoxygeldanamycin (17-AAG). Similar to geldanamycin, 17-AAG is an ATP competitive inhibitor of HSP90 (Schnur et al., 1995). 17-AAG inhibits the chaperone function of HSP90 by mimicking ATP and occupying its place in the N-terminal ATP-ADP-binding pocket (Prodromou et al., 1997). Binding of 17-AAG to the ATP pocket in HSP90 results in an immature HSP90•client complex. Hence, the HSP90 inhibitor interrupts the maturation and proper folding of the client protein by HSP90 leading to the proteasomal

degradation of the client substrates (Neckers and Neckers, 2002; Whitesell and Lindquist, 2005). However, binding of 17-AAG, or any other HSP90 inhibitor to the ATP pocket of the chaperone, elicits a stress response resulting in the transcription activation of HSPs through heat shock factor (HSF-1) (Bagatell et al., 2000). HSF-1 is a transcription activator of all HSP genes (Wu, 1995). Under basal physiological conditions, HSP90 and other cochaperones that are part of the repressing complex are bound to the transcription factor HSF-1, regulating its activation (Guo et al., 2001). The presence of stress inducers in the cell triggers the release of HSF-1 from its constitutive repressing complex triggering transcription of the HSPs. Once released, HSF-1 trimerizes and is phosphorylated resulting in its active conformation (Wu, 1995). Once activated the HSF-1 trimer translocates to the nucleus where it binds the heat shock elements present in the promoter of the HSP genes resulting in an overexpression of HSP proteins in the cell (Baler et al., 1993). The antiapoptotic nature of the HSPs (Beere et al., 2000; Pandey et al., 2000) allows the cell to evade cell death and become resistant to therapeutic agents. Multiple studies have reported that HSP overexpression facilitates resistance to chemotherapeutic agent-induced cytotoxicity in various malignancies (Demidenko et al., 2006; Martins et al., 2008).

The nucleoside analogue 8-Cl-Ado is phosphorylated into its cytotoxic triphosphate 8-Cl-ATP. The accumulation of the cytotoxic metabolite results in a parallel decrease of the ATP cellular pools (Gandhi et al., 2001; Chen et al., 2009). 8-Cl-Ado gets incorporated into RNA during transcription hindering this process (Stellrecht et al., 2003). In addition, this triphosphate inhibits ATP-dependent poly(A) tail synthesis, and as a consequence mRNA processing is inhibited (Chen and Sheppard, 2004; Chen et al., 2010) resulting in *in vitro* cytotoxicity in several solid and hematological malignancies (Gandhi et al., 2001; Balakrishnan et al., 2005). This agent is currently in phase I clinical trials for the treatment of chronic lymphocytic leukemia.

HSP90 is overexpressed in several malignancies including multiple myeloma (MM) (Whitesell and Lindquist, 2005; Chatterjee et al., 2007; Richardson et al., 2011). Inhibition of

heat shock protein 90 (HSP90) is a therapeutic strategy for the treatment of myeloma and other cancers. Based on the mechanism of action of 8-Cl-Ado, we hypothesized that 8-Cl-ATP will inhibit 17-AAG-mediated transcription activation of HSPs, will inhibit client protein translation, and may have more binding of 17-AAG to HSP90 due to ATP decline. Using three multiple myeloma cell lines as a model we tested our hypothesis by combining 8-Cl-Ado with 17-AAG.

## Materials and Methods

**Cell lines.** MM.1S cell line was obtained from Drs. Nancy Krett and Steve Rosen (Robert H. Lurie Comprehensive Cancer Center, Northwestern University, Chicago, IL, USA). U266 and RPMI-8226 cell lines were obtained from Dr. William S. Dalton (H. Lee Moffitt Cancer Center and Research Institute, Tampa, FL, USA). The cell lines were maintained in RPMI-1640 medium (Life Technologies, Inc, Grand Island, NY, USA) supplemented with 10% heat-inactivated fetal bovine serum (Fisher Scientific, Pittsburgh, PA, USA) in the presence of 5% CO<sub>2</sub> at 37°C. Approximate doubling times for MM.1S, U266, and RPMI-8226 are 48, 36, and 24 h, respectively. Cells were routinely tested for *Mycoplasma* infection using a commercially available kit (Gen-Probe Inc, San Diego, CA, USA).

**Materials.** 17-AAG was purchased from Sigma-Aldrich Co. (St Louis, MO, USA) and dissolved in dimethylsulfoxide at a concentration of 1 mM. 8-CI-Ado was obtained from Dr. Vishnuvajjala Rao (Drug Development Branch, National Cancer Institute, Bethesda, MD, USA) and dissolved in Milli-Q water (Millipore Corp., Billerica, MA, USA) at a concentration of 10 mM.

**Radioactive uridine and leucine incorporation.** Global RNA synthesis and global protein synthesis were measured using [<sup>3</sup>H]-uridine or [<sup>3</sup>H]-leucine incorporation (37.2 Ci/mmol or 149Ci/mmol; Moraveck Biochemical Inc, Brea, CA, USA), respectively, as described before (Cervantes-Gomez et al., 2009). Briefly, myeloma cells were left untreated or treated according to the drug schedule. Forty-five minutes prior to the end of incubation, the cells were labeled with the radioactive material at 37°C. The labeled samples were harvested, washed with cold PBS and transferred to glass fiber filters (Whatman Inc, Clifton, NJ, USA) using a Millipore vacuum manifold (Fisher Scientific). The filters were then washed with cold 0.4N perchloric acid and rinsed once with 70% ethanol and dried overnight. The dried filters were transferred to scintillation vials containing 7 mL of high flash point cocktail scintillation fluid (Research Products International Corp, Mount Prospect, IL, USA). Data were expressed as a percentage of untreated control.

**Isolation of RNA and quantitative real time RT-PCR.** Total RNA was isolated using the RNeasy Mini kit (Qiagen, Valencia, CA, USA). The relative transcript levels of gene expression were assessed using TaqMan One Step RT-PCR master mix reagents (Applied Biosystems, Foster City, CA, USA). Predesigned primers and TaqMan probes for glyceraldehyde-3-phosphate dehydrogenase (GAPDH), HSP90 $\alpha$  (HS00743767\_sH), HSP90 $\beta$  (HS00607336\_gH), HSP70 (HS00359147\_s1), HSC70 (HS01683591\_g1), HSP27 (HS00356629\_g1), Akt1 (HS00920503\_m1), STAT-3 (HS01047579\_m1), and Raf-1 (HS00991918\_m1) were purchased from Applied Biosystems. Contaminating DNA was removed from RNA preparations by using a commercially available RNase-free DNase treatment and removal kit (Ambion, Austin, TX, USA). Relative levels of gene expression were determined by using standard curves and normalized with the endogenous gene GAPDH. Experiments were done in triplicate and the results were plotted as fold change in comparison to untreated cells.

**Protein extraction and immunoblot assays.** Following treatment, cells were lysed, protein concentration was determined, and immunoblot analyses were performed as previously described (Cervantes-Gomez et al., 2009). Briefly, myeloma cells were treated as already mentioned; samples were harvested, centrifuged and washed twice with PBS. Cells were lysed using one tablet of Complete Mini Protease Inhibitor Cocktail (Roche, Indianapolis, IN, USA) in 10mL of M-PER Mammalian Protein Extraction Reagent manufactured by Pierce (Rockford, IL, USA). For immunoblot analysis, protein samples were eletrophoresed on Criterion Bis-Tris Gels using the XT MOPS buffer kit (Biorad, Hercules, CA, USA) and transferred to nitrocellulose membranes. Primary antibodies were purchased from the following sources: HSP90 $\alpha/\beta$ , HSP70, HSC70, and HSP27 (Stressgen, Ann Harbor, MI, USA); STAT3, Akt, and GAPDH (Cell Signaling Technology, Beverly, MA, USA); c-Raf (BD Biosciences Pharmingen, San Jose, CA, USA);  $\beta$ -actin (Sigma, Saint Louis, MO, USA); RNA Polymerase II (Covance, Berkeley, CA, USA).



**Immunoprecipitation of HSP90 protein bound to [<sup>3</sup>H]17-AAG.** Radioactive [allylamino-2, 3-<sup>3</sup>H]-17-AAG was synthesized by Moravek Biochemicals. MM.1S cells were incubated with [allylamino-2, 3-<sup>3</sup>H]-17-AAG in the presence or absence of 8-Cl-Ado for 20 h. Cells were lysed by sonication, samples were precleared and protein concentration was determined. One mg of protein per sample was incubated for 2 h at 4°C with 20 µg of HSP90α/β along with proper controls. Protein G Plus/Protein A-Agarose was added to each sample and incubated for 1 h at 4°C. Samples were centrifuged and the immuno-radiolabeled precipitants washed. The [allylamino-2, 3-<sup>3</sup>H]-17-AAG bound to HSP90α/β was determined by a liquid scintillation counter.

**Annexin V cell death assay.** Myeloma cells were treated with the drugs as described, harvested and incubated with 7-AAD and Annexin V-FITC (BD Biosciences Pharmingen). Total cell death was analyzed using the BD FACSCalibur system (BD Biosciences). The expected percentage of cells surviving after treatment with the combination was calculated using the fractional two-drug combinational analysis. This compares the expected and observed (Annexin V/7-AAD staining) levels of cell death in the combination treatment. The percentage of cells surviving 17-AAG treatment (100% - X% Annexin V/7-AAD staining) was multiplied by the percentage of cells surviving 8-Cl-Ado treatment (100% - X% Annexin V/7-AAD staining) divided by 100.

**Quantitation of intracellular nucleotides.** After treatment cells were harvested and a perchloric acid extraction was performed as previously described (Gandhi et al., 2001). Nucleotide separation and quantitation were performed using high pressure liquid chromatography (HPLC) as described before (Gandhi et al., 2001).

**Statistical analysis.** One-tailed paired Student's *t*-test analyses were done using GraphPad Prism (GraphPad Software, San Diego, CA, USA).

## Results

**Experimental design.** Myeloma cells (MM.1S, RPMI-8226, and U266) were either untreated or treated with 0.5  $\mu$ M 17-AAG alone for 8 h, a combination treatment with 10  $\mu$ M 8-Cl-Ado for 12 h followed by 0.5  $\mu$ M 17-AAG for 8 h, or 10  $\mu$ M 8-Cl-Ado alone for 20 h. These concentrations were selected based on prior reports and are clinically achievable (Gandhi et al., 2001; Cervantes-Gomez et al., 2009). Two additional combination sequences were also evaluated. In one strategy, cells were treated with 0.5  $\mu$ M 17-AAG alone for 20 h, a combination treatment with 0.5  $\mu$ M 17-AAG added first for 8 h followed by 10  $\mu$ M 8-Cl-Ado for 12 h, or 10  $\mu$ M 8-Cl-Ado alone for 12 h. The last combination approach evaluated 10  $\mu$ M 8-Cl-Ado and 0.5  $\mu$ M 17-AAG added simultaneously for 20 h, including the two parallel conditions with the single agents alone.

**Cytotoxicity of 8-Cl-Ado in combination with 17-AAG in myeloma cells.** Endogenous cell death was subtracted from each condition. Treatment with 17-AAG resulted in <5% cell death while with 8-Cl-Ado resulted in 26, 6 and 2% death in MM.1S, RPMI-8226, and U266 cells, respectively. In the same cell lines, the combination resulted in 55, 15, and 19% cell death (Table 1). The measured (observed) cytotoxicity for the combination condition was more than the expected (calculated) cell death and was significantly different in all cell lines (MM.1S,  $p = 0.019$ ; RPMI-8226,  $p = 0.011$ ; U266,  $p = 0.019$ ). Since these results suggested more than additive effect, different combination sequences for 8-Cl-Ado and 17-AAG were tested for cytotoxicity (data not shown). The cytotoxicity between the expected and observed cell death values was either not different or marginally different in the simultaneous combination of both drugs (MM.1S,  $p = 0.045$ ; RPMI-8226,  $p = 0.29$ ; U266,  $p = 0.047$ ).

**Effect of 8-Cl-Ado on global RNA synthesis.** MM.1S cell line was more sensitive to the RNA inhibitory actions of 8-Cl-Ado than RPMI-8226. A 25% decrease in global RNA synthesis was observed after 4 h, further decreasing to 50% after 8 h. Treatment with 8-Cl-Ado

in RPMI-8226 cells caused only a 25% inhibition at both time points compared to control (data not shown).

**Effect of 8-Cl-Ado and 17-AAG on constitutive and stress-inducible HSP mRNAs.**

Treatment with 17-AAG triggered the elevation of all constitutive and stress-inducible *HSP* mRNA ranging from more than 3-fold to 9-fold (Fig 1). However, this induction persisted with the combination treatment in both cell lines, which implies that 8-Cl-Ado was not able to abrogate the *HSP*-induction elicited by 17-AAG (Fig 1A-B, D). In fact, the combination treatment further elevated the levels of *HSP70* by 13- and 4-fold in MM.1S and RPMI-8226 cells, respectively (Fig 1C). Similarly, in MM.1S the mRNA levels of *HSP27* were further induced in the combination treatment (Fig 1E,  $p = 0.02$ ). In RPMI-8226 cells treatment with 17-AAG alone resulted in an 8-fold increase of *HSP27* transcript levels that remained similar after 8-Cl-Ado addition (Fig 1E). Treatment with 8-Cl-Ado as a single agent did not result in a decrease in the basal levels of any of the inducible or constitutive *HSP* transcript levels (Fig 1A-E).

**Effect of 8-Cl-Ado on constitutive and stress-inducible HSP expression levels induced by 17-AAG.** Immunoblots were performed to determine if the observed increase in inducible *HSP* transcripts after combination treatment were obtained at the protein level (Fig 2). *HSP70* and *HSP27* protein levels were increased with 17-AAG treatment in MM cells (Fig 2A). Similar to *HSP* transcript levels, 17-AAG-induced expression of HSPs was not abrogated by 8-Cl-Ado addition. Treatment of 8-Cl-Ado alone did not affect the endogenous levels of HSPs in any cell line. The normalization, quantitation and statistical analyses of three independent immunoblots indicated that 8-Cl-Ado was not able to abrogate 17-AAG-mediated induction of HSPs (Fig 2B).

**Effect of 8-Cl-Ado and 17-AAG alone and in combination on client protein expression levels.** Oncoproteins, such as STAT-3, Raf-1, and Akt, are part of redundant signaling cascades. 17-AAG and other HSP90 inhibitors are unique in their ability to simultaneously down-regulate numerous client oncoprotein substrates by increasing their

turnover rate (Neckers and Neckers, 2002). 8-Cl-Ado can inhibit transcription and translation processes due to its actions not only on RNA incorporation and termination but also on the decrease of endogenous ATP pool levels (Gandhi et al., 2001; Stellrecht et al., 2003; Chen et al., 2009). The combination of both agents resulted in a drastic decrease (>75%) of STAT-3, Raf-1, and Akt compared to untreated control as well as the single agents in MM.1S and U226 cells, this decrease was minimal in the RPMI-8226 cell line (Fig 3A). Three independent immunoblots showed that the combination of 8-Cl-Ado and 17-AAG resulted in a statistically significant decrease of STAT3, Raf-1, and Akt client protein levels in all the evaluated MM cell lines when compared to the untreated control, with the only exception of Raf-1 protein levels in RPMI-8226 cells (Fig 3B).

**Effect of 8-Cl-Ado and 17-AAG alone and in combination on STAT3, Raf-1, and Akt mRNA levels.** To investigate if the reduction in STAT-3, Raf-1, and Akt expression observed in the combination treatment was due to a decrease in their mRNA levels, real time RT-PCR was performed (Fig 4). There was not a significant change in STAT3 (Fig 4A), Raf-1 (Fig 4B), or Akt (Fig 4C) transcript levels with any of the treatments in neither cell line. Although there was a small induction of Akt transcript in RPMI-8226, this proved to be significant ( $p = 0.02$ , Fig 4C). Therefore, the decrease in STAT3, Raf-1, and Akt protein levels in the combination treatment is not due to a change in their transcript levels.

**Cellular metabolism of 8-Cl-Ado and its effect on the binding of [<sup>3</sup>H] 17-AAG to HSP90.** In MM.1S cells, a parallel decrease in ATP pools is observed with accumulation of 8-Cl-ATP. After the first 2 h of treatment with 8-Cl-Ado, there is 100  $\mu$ M 8-Cl-ATP accumulation with a 25% decrease in ATP levels. By 20 h, treatment with 8-Cl-Ado decreases ATP levels by 65%, with approximately 1 mM intracellular ATP remaining.

In order to determine if addition of 17-AAG affected the accumulation of 8-Cl-ATP or the decrease in ATP pool, the combination condition was also evaluated (Fig 5B,C). Treatment with 8-Cl-Ado caused a 57% decrease in ATP levels. The combination treatment resulted in an 83%

drop of the ATP pool. Surprisingly, the expected parallel accumulation of 8-Cl-ATP levels was not observed. Addition of 17-AAG after 8-Cl-Ado treatment resulted in only 203  $\mu\text{M}$  8-Cl-ATP accumulation in the combination treatment compared to 607  $\mu\text{M}$  8-Cl-ATP after 8-Cl-Ado treatment (Fig 5B).

In RPMI-8226 cells, after 8-Cl-Ado treatment, 8-Cl-ATP accumulation reached 1109  $\mu\text{M}$  with a slight decrease in ATP pool. Addition of 17-AAG following 8-Cl-Ado treatment did not affect the levels of ATP to a great extent compared with 8-Cl-Ado alone (76% vs. 64%). However, a decrease in 8-Cl-ATP levels was also observed when compared to 8-Cl-Ado treatment alone (Fig 5B). Overall these data suggests that 17-AAG affects the metabolism of 8-Cl-Ado to its cytotoxic triphosphate form.

In order to bind to HSP90, 17-AAG competes with ATP (Schnur et al., 1995) inhibiting the stabilization of client proteins by HSP90 resulting in client protein proteasomal degradation (Neckers and Neckers, 2002). The combination treatment resulted in a dramatic decrease in ATP levels compared to treatment with 8-Cl-Ado alone (Fig 5C) as well as a marked decreased in the client proteins levels (Fig 3). A possible explanation for this could be that there is more binding of 17-AAG to HSP90 in the combination treatment since 8-Cl-Ado decreases cellular ATP pool. For this reason, Immunoprecipitation and immunoblot analyses of radioactive [ $^3\text{H}$ ]17-AAG bound to HSP90 were performed in MM.1S cells for the combination treatment of 8-Cl-Ado and [ $^3\text{H}$ ]17-AAG compared to [ $^3\text{H}$ ]17-AAG treatment alone (Fig 5D). MM.1S cells were treated with 0.5  $\mu\text{M}$  [ $^3\text{H}$ ]17-AAG alone or the combination of 10 $\mu\text{M}$  8-Cl-Ado plus [ $^3\text{H}$ ]17-AAG for 20 h. Each condition was performed twice in duplicate. The total amount of [ $^3\text{H}$ ]17-AAG in both condition treatments was similar (175000 DPM). Immunoprecipitation of HSP90 $\alpha/\beta$  in MM.1S cells treated with [ $^3\text{H}$ ]17-AAG alone determined that [ $^3\text{H}$ ]17-AAG is bound to HSP90 $\alpha/\beta$  and the complex can be pulled down and radioactivity analyzed (approximately 25000 DPM). However, the combination condition did not show an increasing amount of [ $^3\text{H}$ ]17-AAG binding to HSP90 $\alpha/\beta$ . In addition, immunoprecipitation of RNA Pol II protein indicated the absence of

[<sup>3</sup>H]17-AAG bound to RNA Pol II since the radioactive count was determined to be around 50 DPM. These data indicate that a 57% decrease in ATP levels due to 8-Cl-Ado treatment (Fig 5A,C) does not increase the amount of [<sup>3</sup>H]17-AAG binding to HSP90α/β protein (Fig 5D).

**Global protein synthesis and role of protein 4E-BP1.** The effect of 8-Cl-Ado alone and in combination with 17-AAG on global protein synthesis (Fig 6A) and the phosphorylation status of 4E-BP1 (Fig 6B), a repressor protein of mRNA translation, was analyzed. Radioactive leucine incorporation in untreated MM.1S and U266 cells had an average of 19776 and 21635 DPM, respectively. The global protein synthesis was decreased by <30% with 8-Cl-Ado treatment in both cell lines. However, the combination treatment resulted in a 50% decline of leucine incorporation compared to the untreated control in MM.1S cells, though no further decrease was observed in U266 cells. MM.1S cells were treated with 10 μM 8-Cl-Ado for different time points or starved for several days to be used as a positive control for hypophosphorylation of 4E-BP1 and U266 cells were treated with the two different sequential or simultaneous combinations of 8-Cl-Ado and 17-AAG to determine if 17-AAG could further affect the phosphorylation status of 4E-BP1 (Fig 6B). The multiple bands of 4E-BP1 represent its varied phospho-forms, and stacking of the bands represents its hypophosphorylated form (Gingras et al., 1998; Gingras et al., 2001). MM.1S cells treated with 8-Cl-Ado resulted in a time dependent decrease in 4E-BP1 phosphorylation levels, with a more pronounced hypophosphorylated form of 4E-BP1 appearing at 24, 48 and 72 h. In U266 cells, treatment with 17-AAG for 8 or 20 h did not affect the hyperphosphorylation status of 4E-BP1 as shown by its multiple bands. Treatment with 8-Cl-Ado for 12 or 20 h resulted in a decrease in phosphorylation levels in 4E-BP1. However, combination treatment with 8-Cl-Ado and 17-AAG resulted in further hypophosphorylation of 4E-BP1 as shown by the absence of multiple bands. As expected, starvation of MM.1S cells (positive control) for 24 and 48 h resulted in hypophosphorylation of 4E-BP1.

## Discussion

Inhibition of heat shock protein 90 (HSP90) is an attractive therapeutic strategy for the treatment of myeloma. Preclinical and clinical studies suggest that HSP90 inhibitors increase cytotoxic susceptibility in myeloma cells when combined with other forms of therapy such as conventional chemotherapy, radiation, or targeted therapy (Richardson et al., 2011). The ability of 8-Cl-Ado to inhibit 17-AAG-mediated transcription induction of HSPs leading to increased cytotoxicity was evaluated based on the following mechanisms of action of this ATP analog (Stellrecht et al., 2003; Chen and Sheppard, 2004; Chen et al., 2010). First, the cytotoxic metabolite of 8-Cl-Ado, 8-Cl-ATP, can be incorporated into the body of RNA leading to mRNA synthesis inhibition (Stellrecht et al., 2003). Second, 8-Cl-Ado treatment depletes cellular ATP pools in several cell lines such as breast cancer (Stellrecht et al., 2010), mantle cell lymphoma, and multiple myeloma (Gandhi et al., 2001), as well as primary chronic lymphocytic leukemia cells (Balakrishnan et al., 2005). ATP is a substrate for RNA synthesis and hence its decline will affect transcription. Third, 8-Cl-ATP can inhibit mammalian polyadenylation a required step for transcript function and stability (Chen and Sheppard, 2004; Chen et al., 2010).

Therefore, due to its inhibitory actions on RNA synthesis and stability, 8-Cl-Ado was selected as the agent to combine with 17-AAG. However, real-time RT-PCR data demonstrated that 8-Cl-Ado was not able to inhibit the transcription of any of the stress-inducible or constitutive HSP mRNA levels (Fig 1), rather there was an induction of *HSP70* mRNA level when 8-Cl-Ado and 17-AAG drugs were combined (Fig 1C). As previously mentioned, *HSP70* gene has some singularities that distinguish it from the rest of the HSP genes. It is primed for rapid induction since *HSP70* transcription is initiated and paused until HSF-1 relieves this pause when the cell undergoes some kind of stress (Lis and Wu, 1993). Studies investigating the induction of the HSP response in *Drosophila* and humans have reported that a decrease in the intracellular ATP pools stimulates the binding of HSF-1 to the *HSP70* DNA promoter, although this is not sufficient to trigger *HSP70* transcription (Winegarden et al., 1996). However, a second

stimulus (such as 17-AAG treatment) augments the heat shock stress response resulting in elevated induction of *HSP70* mRNA (Bagatell et al., 2000). One of the mechanisms by which 8-CI-Ado exerts cytotoxicity is through depletion of the ATP pools; hence these observations may explain why the combination of 8-CI-Ado followed by 17-AAG results in an increased level of HSP70 mRNA.

Similar to HSP transcripts, myeloma cells treated with 8-CI-Ado did not indicate a reduction on STAT3, Raf-1, or Akt mRNA levels (Fig 4). A possible explanation for the inability of 8-CI-Ado to decrease HSP or client protein mRNA levels is that the length of the transcript could be an important feature. For example, HSP70, HSP27, and Raf-1 transcript length is reported to be 2.2, 2.2, and 2.8 Kb, respectively (Hunt and Morimoto, 1985). In contrast, c-Met, an oncogene whose expression promotes tumorigenesis in multiple human cancers, is 8 Kb long (Miller et al., 1996). The c-Met transcript is depleted by 8-CI-Ado treatment followed by a reduced protein expression (Stellrecht et al., 2007). Hence, it may be possible that incorporation of 8-CI-ATP is increased with long transcripts leading to its inhibitory actions in mRNA synthesis.

Another possibility is that inducible gene transcription is not affected by transcription inhibition. For example, as described in an earlier report for actinomycin D (Cervantes-Gomez et al., 2009), DRB (Gomes et al., 2006),  $\alpha$ -amanitin (Ljungman et al., 1999), and the cyclin-dependent kinase inhibitor roscovitine (Dey et al., 2008), RNA Pol II inactivation does not always result in transcription inhibition of some of the stress-inducible genes such as HSP70, p53, p21 and PUMA.

For HSPs, a lack of decrease in mRNA level was consistent with a lack of decline of all HSP expression; however, in spite of no change in mRNA levels, a decrease in client protein levels is measured in MM cells after 8-CI-Ado treatment which is further reduced when combined with 17-AAG (Fig 3). 8-CI-Ado-mediated decrease in the endogenous ATP pool (Fig 5A,C) could account for the decrease in client protein levels. The possibility that ATP depletion



could increase binding of 17-AAG to HSP90, increasing the turn-over rate of the client proteins, was contemplated as a potential mechanism of action by which 8-Cl-Ado and 17-AAG combination resulted in more pronounced decrease in client proteins and in increased cell death (Fig 5D). Results indicated that when cells are treated with [<sup>3</sup>H]17-AAG or 8-Cl-Ado in combination with [<sup>3</sup>H]17-AAG there is no further increase in the binding of [<sup>3</sup>H]17-AAG to HSP90. This suggests that the levels of ATP in the cell do not affect binding affinity of [<sup>3</sup>H]17-AAG for HSP90.

Interestingly, a study investigating the effect of ATP depletion in the stabilization of the client protein ErbB2 by HSP90 concluded that a decrease in the levels of ATP results in the disruption of the HSP90•ErbB2 complex and ErbB2 degradation (Peng et al., 2005). The authors of this study lowered ATP concentration in the cell by inhibiting glycolysis and mitochondrial respiration using the pharmacological inhibitors 2-deoxy-D-glucose or antimycin A, respectively. They concluded that depletion of cellular ATP levels alters stabilization and maturation of ErbB2 by HSP90, and this depletion of the client protein ErbB2 was similar to the one obtained when cells were treated with geldanamycin. A similar decrease in protein levels was observed for the other two client proteins evaluated in this study, Raf-1 and Akt, following ATP depletion due to treatment with 2-deoxy-D-glucose or antimycin A. This indicates that a decrease in cellular ATP concentration mimics the mechanism by which HSP90 inhibitors cause cytotoxicity in the cell. Hence, the decrease of client proteins levels observed with 8-Cl-Ado treatment alone could be a result of its effect in ATP depletion.

An additional plausible mechanism by which 8-Cl-Ado could be leading to decreased client protein levels, without affecting transcript levels, is by negatively affecting protein synthesis; a process that requires high cellular energy. Protein translation is regulated when the cell undergoes some kind of stress that perturbs homeostasis, and the mTOR (mammalian target of rapamycin) pathway is sensitive to changes in cellular ATP levels. Protein 4E-BP1 regulates translation, and its activity is in turn regulated by the upstream serine/threonine kinase

mTOR (Gingras et al., 1998). The translation repressing activity of 4E-BP1 is regulated by phosphorylation at 4 specific amino-acid residues (Gingras et al., 1998; Gingras et al., 2001). In its hypophosphorylated state, 4E-BP1 represses initiation of translation by binding to the eukaryotic initiation factor 4E (eIF4) (Gingras et al., 1998). In contrast, hyperphosphorylation of 4E-BP1 by upstream kinases such as mTOR results in the release of eIF4 allowing translation initiation (Gingras et al., 2001). Similar to known inhibitor, starvation, treatment with 8-Cl-Ado results in hypophosphorylation of 4E-BP1 (Fig 6B). The hypophosphorylated status of 4E-BP1 could initially be attributed to the decrease in ATP concentration. This in-principle could decrease kinase activity as a result of substrate availability. However, with another ATP congener, a decline in ATP did not result in a global decrease in protein phosphorylation (Ghias et al., 2005). Additionally, in U266 cells treated with 8-Cl-Ado and 17-AAG in sequential or simultaneous combination, 4E-BP1 was further hypophosphorylated compared to treatment with the drugs as single agents (Fig 6B). Therefore, further studies addressing the effect of 8-Cl-Ado alone and in combination with 17-AAG on 4E-BP1 and global protein translation are needed. Consistent with the consequence of 4E-BP1 hypophosphorylation, there was a global decline in protein synthesis. Although the mechanism by which 8-Cl-Ado treatment leads to hypophosphorylation of the translation repressor 4E-BP1 was not elucidated in this current study, this negative effect on the translation process could be another potential mechanism by which treatment with 8-Cl-Ado affects protein translation.

In summary, although the mechanism by which 8-Cl-Ado and 17-AAG interact remains to be fully elucidated and tested in MM patient samples, the combination of transcription/translation inhibitors that cause ATP depletion such as 8-Cl-Ado could be used in combination with 17-AAG as a strategy to decrease client protein levels resulting in increase cytotoxicity regardless of the high expression levels of the antiapoptotic HSP expression levels. In addition, different time schedules and combination sequences were also evaluated for the two drugs (data not shown) which resulted in a similar molecular and cytotoxic response as the

combination strategy presented in this study. Since the agents evaluated in this investigation are either approved drugs or in clinical trials, these approaches may be applied in the clinic towards the design of new drug combination strategies.

### **Authorship Contributions**

Participated in research design: Cervantes-Gomez, Nimmanapalli, and Gandhi

Conducted experiments: Cervantes-Gomez

Performed data analysis: Cervantes-Gomez and Gandhi

Wrote the manuscript: Cervantes-Gomez and Gandhi

## References

Bagatell R, Paine-Murrieta GD, Taylor CW, Pulcini EJ, Akinaga S, Benjamin IJ and Whitesell L (2000) Induction of a heat shock factor 1-dependent stress response alters the cytotoxic activity of hsp90-binding agents. *Clin Cancer Res* **6**:3312-3318.

Balakrishnan K, Stellrecht CM, Genini D, Ayres M, Wierda WG, Keating MJ, Leoni LM and Gandhi V (2005) Cell death of bioenergetically compromised and transcriptionally challenged CLL lymphocytes by chlorinated ATP. *Blood* **105**:4455-4462.

Baler R, Dahl G and Voellmy R (1993) Activation of human heat shock genes is accompanied by oligomerization, modification, and rapid translocation of heat shock transcription factor HSF1. *Mol Cell Biol* **13**:2486-2496.

Beere HM, Wolf BB, Cain K, Mosser DD, Mahboubi A, Kuwana T, Tailor P, Morimoto RI, Cohen GM and Green DR (2000) Heat-shock protein 70 inhibits apoptosis by preventing recruitment of procaspase-9 to the Apaf-1 apoptosome. *Nat Cell Biol* **2**:469-475.

Biamonte MA, Van de Water R, Arndt JW, Scannevin RH, Perret D and Lee WC (2010) Heat shock protein 90: inhibitors in clinical trials. *J Med Chem* **53**:3-17.

Cervantes-Gomez F, Nimmanapalli R and Gandhi V (2009) Transcription inhibition of heat shock proteins: a strategy for combination of 17-allylamino-17-demethoxygeldanamycin and actinomycin d. *Cancer Res* **69**:3947-3954.

Chatterjee M, Jain S, Stuhmer T, Andrulis M, Ungethum U, Kuban RJ, Lorentz H, Bommert K, Topp M, Kramer D, Muller-Hermelink HK, Einsele H, Greiner A and Bargou RC (2007) STAT3

and MAPK signaling maintain overexpression of heat shock proteins 90alpha and beta in multiple myeloma cells, which critically contribute to tumor-cell survival. *Blood* **109**:720-728.

Chen LS, Du-Cuny L, Vethantham V, Hawke DH, Manley JL, Zhang S and Gandhi V (2010) Chain termination and inhibition of mammalian poly(A) polymerase by modified ATP analogues. *Biochem Pharmacol* **79**:669-677.

Chen LS, Nowak BJ, Ayres ML, Krett NL, Rosen ST, Zhang S and Gandhi V (2009) Inhibition of ATP synthase by chlorinated adenosine analogue. *Biochem Pharmacol* **78**:583-591.

Chen LS and Sheppard TL (2004) Chain termination and inhibition of *Saccharomyces cerevisiae* poly(A) polymerase by C-8-modified ATP analogs. *J Biol Chem* **279**:40405-40411.

Demidenko ZN, Vivo C, Halicka HD, Li CJ, Bhalla K, Broude EV and Blagosklonny MV (2006) Pharmacological induction of Hsp70 protects apoptosis-prone cells from doxorubicin: comparison with caspase-inhibitor- and cycle-arrest-mediated cytoprotection. *Cell Death Differ* **13**:1434-1441.

Dey A, Wong ET, Cheek CF, Tergaonkar V and Lane DP (2008) R-Roscovitine simultaneously targets both the p53 and NF-kappaB pathways and causes potentiation of apoptosis: implications in cancer therapy. *Cell Death Differ* **15**:263-273.

Gandhi V, Ayres M, Halgren RG, Krett NL, Newman RA and Rosen ST (2001) 8-chloro-cAMP and 8-chloro-adenosine act by the same mechanism in multiple myeloma cells. *Cancer Res* **61**:5474-5479.

Ghias K, Ma C, Gandhi V, Plataniias LC, Krett NL and Rosen ST (2005) 8-Amino-adenosine induces loss of phosphorylation of p38 mitogen-activated protein kinase, extracellular signal-regulated kinase 1/2, and Akt kinase: role in induction of apoptosis in multiple myeloma. *Mol Cancer Ther* **4**:569-577.

Gingras AC, Kennedy SG, O'Leary MA, Sonenberg N and Hay N (1998) 4E-BP1, a repressor of mRNA translation, is phosphorylated and inactivated by the Akt(PKB) signaling pathway. *Genes Dev* **12**:502-513.

Gingras AC, Raught B, Gygi SP, Niedzwiecka A, Miron M, Burley SK, Polakiewicz RD, Wyslouch-Cieszyńska A, Aebersold R and Sonenberg N (2001) Hierarchical phosphorylation of the translation inhibitor 4E-BP1. *Genes Dev* **15**:2852-2864.

Gomes NP, Bjerke G, Llorente B, Szostek SA, Emerson BM and Espinosa JM (2006) Gene-specific requirement for P-TEFb activity and RNA polymerase II phosphorylation within the p53 transcriptional program. *Genes Dev* **20**:601-612.

Guo Y, Guettouche T, Fenna M, Boellmann F, Pratt WB, Toft DO, Smith DF and Voellmy R (2001) Evidence for a mechanism of repression of heat shock factor 1 transcriptional activity by a multichaperone complex. *J Biol Chem* **276**:45791-45799.

Hartl FU and Hayer-Hartl M (2002) Molecular chaperones in the cytosol: from nascent chain to folded protein. *Science* **295**:1852-1858.

Hunt C and Morimoto RI (1985) Conserved features of eukaryotic hsp70 genes revealed by comparison with the nucleotide sequence of human hsp70. *Proc Natl Acad Sci U S A* **82**:6455-6459.

Lis J and Wu C (1993) Protein traffic on the heat shock promoter: parking, stalling, and trucking along. *Cell* **74**:1-4.

Ljungman M, Zhang F, Chen F, Rainbow AJ and McKay BC (1999) Inhibition of RNA polymerase II as a trigger for the p53 response. *Oncogene* **18**:583-592.

Martins AS, Ordonez JL, Garcia-Sanchez A, Herrero D, Sevillano V, Osuna D, Mackintosh C, Caballero G, Otero AP, Poremba C, Madoz-Gurpide J and de Alava E (2008) A pivotal role for heat shock protein 90 in Ewing sarcoma resistance to anti-insulin-like growth factor 1 receptor treatment: in vitro and in vivo study. *Cancer Res* **68**:6260-6270.

Miller RT, Glover SE, Stewart WS, Corton JC, Popp JA and Cattley RC (1996) Effect on the expression of c-met, c-myc and PPAR-alpha in liver and liver tumors from rats chronically exposed to the hepatocarcinogenic peroxisome proliferator WY-14,643. *Carcinogenesis* **17**:1337-1341.

Neckers L and Neckers K (2002) Heat-shock protein 90 inhibitors as novel cancer chemotherapeutic agents. *Expert Opin Emerg Drugs* **7**:277-288.

Onuoha SC, Coulstock ET, Grossmann JG and Jackson SE (2008) Structural studies on the co-chaperone Hop and its complexes with Hsp90. *J Mol Biol* **379**:732-744.



Pandey P, Farber R, Nakazawa A, Kumar S, Bharti A, Nalin C, Weichselbaum R, Kufe D and Kharbanda S (2000) Hsp27 functions as a negative regulator of cytochrome c-dependent activation of procaspase-3. *Oncogene* **19**:1975-1981.

Peng X, Guo X, Borkan SC, Bharti A, Kuramochi Y, Calderwood S and Sawyer DB (2005) Heat shock protein 90 stabilization of ErbB2 expression is disrupted by ATP depletion in myocytes. *J Biol Chem* **280**:13148-13152.

Pratt WB and Toft DO (2003) Regulation of signaling protein function and trafficking by the hsp90/hsp70-based chaperone machinery. *Exp Biol Med (Maywood)* **228**:111-133.

Prodromou C, Roe SM, O'Brien R, Ladbury JE, Piper PW and Pearl LH (1997) Identification and structural characterization of the ATP/ADP-binding site in the Hsp90 molecular chaperone. *Cell* **90**:65-75.

Richardson PG, Mitsiades CS, Laubach JP, Lonial S, Chanan-Khan AA and Anderson KC (2011) Inhibition of heat shock protein 90 (HSP90) as a therapeutic strategy for the treatment of myeloma and other cancers. *Br J Haematol* **152**:367-379.

Schnur RC, Corman ML, Gallaschun RJ, Cooper BA, Dee MF, Doty JL, Muzzi ML, DiOrio CI, Barbacci EG, Miller PE and et al. (1995) erbB-2 oncogene inhibition by geldanamycin derivatives: synthesis, mechanism of action, and structure-activity relationships. *J Med Chem* **38**:3813-3820.

Sharp S and Workman P (2006) Inhibitors of the HSP90 molecular chaperone: current status. *Adv Cancer Res* **95**:323-348.

Smith DF, Sullivan WP, Marion TN, Zaitso K, Madden B, McCormick DJ and Toft DO (1993) Identification of a 60-kilodalton stress-related protein, p60, which interacts with hsp90 and hsp70. *Mol Cell Biol* **13**:869-876.

Stellrecht CM, Ayres M, Arya R and Gandhi V (2010) A unique RNA-directed nucleoside analog is cytotoxic to breast cancer cells and depletes cyclin E levels. *Breast Cancer Res Treat* **121**:355-364.

Stellrecht CM, Phillip CJ, Cervantes-Gomez F and Gandhi V (2007) Multiple myeloma cell killing by depletion of the MET receptor tyrosine kinase. *Cancer Res* **67**:9913-9920.

Stellrecht CM, Rodriguez CO, Jr., Ayres M and Gandhi V (2003) RNA-directed actions of 8-chloro-adenosine in multiple myeloma cells. *Cancer Res* **63**:7968-7974.

Whitesell L and Lindquist SL (2005) HSP90 and the chaperoning of cancer. *Nat Rev Cancer* **5**:761-772.

Winegarden NA, Wong KS, Sopta M and Westwood JT (1996) Sodium salicylate decreases intracellular ATP, induces both heat shock factor binding and chromosomal puffing, but does not induce hsp 70 gene transcription in *Drosophila*. *J Biol Chem* **271**:26971-26980.

Wu C (1995) Heat shock transcription factors: structure and regulation. *Annu Rev Cell Dev Biol* **11**:441-469.

## Footnotes

This work was supported by National Institutes of Health National Cancer Institute Grants Lymphoma SPORE [CA136411] and Myeloma SPORE [CA142509].

## Legends for Figures

**Figure 1. Effect of 8-CI-Ado, 17-AAG, or their combination on constitutive and stress-inducible HSP mRNA in MM cells.** Inducible HSP90 $\alpha$  (A), constitutive HSP90 $\beta$  (B), inducible HSP70 (C), constitutive HSC70 (D), and HSP27 (E) mRNA levels were measured using real-time RT-PCR. GAPDH was used for normalization. mRNA levels are plotted as fold change in comparison with the untreated control. Each column represents the mean  $\pm$  SD of triplicate experiments. Statistical values comparing 17-AAG alone with the combination condition are shown.

**Figure 2. Effect of 8-CI-Ado and 17-AAG alone and in combination on HSP expression levels in MM cells.** (A) Immunoblots were performed and antibodies for inducible HSP90 $\alpha$  and constitutive HSP90 $\beta$ , inducible HSP70, constitutive HSC70, HSP27, and the loading control  $\beta$ -actin in MM.1S, RPMI-8226 and U266 cells. (B) Immunoblot assays were performed in triplicate and quantified using Odyssey infrared imaging system application software. Protein levels of constitutive and stress-inducible HSP were normalized to  $\beta$ -actin. Data represents three independent immunoblots plotted as mean  $\pm$  SD. Statistical values comparing 17-AAG alone with the combination condition are shown.

**Figure 3. Effect of 8-CI-Ado and 17-AAG alone and in combination on STAT3, Raf-1, and Akt client protein expression levels in MM cells.** (A) Immunoblots were performed to detect protein levels for STAT3, Raf-1, Akt, and the loading control  $\beta$ -actin in MM.1S, RPMI-8226, and U266 cells. (B) Immunoblots were performed in triplicate and quantified using Odyssey infrared imaging system application software. Protein levels for STAT3, Raf-1, and Akt were normalized to  $\beta$ -actin. Data represents three independent immunoblots plotted as mean  $\pm$  SD. Statistical

values comparing the combination condition with 17-AAG alone, 8-Cl-Ado alone, or the untreated control are shown.

**Figure 4. Effect of 8-Cl-Ado and 17-AAG alone and in combination on STAT3, Raf-1, and Akt client protein mRNA levels in MM.1S and RPMI-8226 cells.** STAT3 (A), Raf-1 (B), and Akt (C) mRNA levels were measured using real-time RT-PCR and represented as fold change in comparison with the untreated control. GAPDH was used as the endogenous gene for normalization and each column represents the mean  $\pm$  SD of triplicate experiments. Statistical values comparing the combination condition with 17-AAG alone, 8-Cl-Ado alone, or the untreated control are shown.

**Figure 5. Cellular metabolism of 8-Cl-Ado and its effect on the binding of [<sup>3</sup>H] 17-AAG to HSP90.** (A) Accumulation of 8-Cl-ATP and concomitant ATP concentration decrease. MM.1S cells were treated with 10  $\mu$ M 8-Cl-Ado as a function of time. Cells were harvested at the indicated times and 8-Cl-ATP ( $\Delta$ ) and ATP ( $\bullet$ ) levels in the cells were measured. Each time point was performed in triplicate and data represented as mean  $\pm$  SD. (B-C) 8-Cl-Ado metabolism to 8-Cl-ATP and ATP accumulation in the absence or presence of 17-AAG. (D) Immunoprecipitation of HSP90 bound to [<sup>3</sup>H] 17-AAG. MM.1S cells were treated with 0.5  $\mu$ M [<sup>3</sup>H] 17-AAG in the absence or presence of 8-Cl-Ado for 20 h then lysed and immunoprecipitated for HSP90. Similar experiments were performed using RNA Pol II as a negative control for non-specific [<sup>3</sup>H]-17-AAG binding. Each column represents the mean  $\pm$  SD of two independent experiments done in duplicate.

**Figure 6. Global protein synthesis and 4E-BP1 role.** (A) Radioactive leucine incorporation after treatment with 8-Cl-Ado or combination. Data were plotted as the percentage of untreated control and represents the mean  $\pm$  SD of three independent experiments each done in

duplicate. (B) Effect of 8-Cl-Ado on 4E-BP1 phosphorylation status MM.1S cells were treated with 10  $\mu$ M 8-Cl-Ado for the indicated times and immunoblots were performed. U266 cells were either left untreated (U) or treated with 17-AAG for 8 h, the combination of 8-Cl-Ado for 12 h followed by 17-AAG for 8 h, 8-Cl-Ado for 20 h, 17-AAG for 20 h, the combination of 17-AAG for 12 h followed by 8-Cl-Ado for 8 h, 10  $\mu$ M 8-Cl-Ado for 12 h, or the combination of 8-Cl-Ado and 17-AAG added simultaneously for 20 h. Cells were harvested and immunoblots were performed and analyzed with antibodies detecting for 4E-BP1 and the loading control  $\beta$ -actin. MM.1S cells were starved for the indicated times to use a positive control for dephosphorylation of 4E-BP1.

**Tables**

**Table I.** Cytotoxicity of 8-Cl-Ado followed by 17-AAG combination sequence in MM cell lines.

Cell death was measured by flow cytometry and determined as the percentage of cells staining positive for Annexin V/7-AAD after subtracting the percentage of endogenous cell death (which was <18%). The expected percent survival for the combination condition was calculated following the fractional two-drug combination analysis as described in materials and methods. *P* values are comparing expected with observed cell death.

<b>8-Cl-Ado</b> → <b>17-AAG</b>	<b>17-AAG</b>	<b>8-Cl-Ado</b>	<b>Combination</b>	
	<b>0.5 μM</b> <i>8 h</i>	<b>10 μM</b> <i>20 h</i>	<i>Expected</i>	<i>Observed</i>
<b>MM.1S</b>				
<i>Cell Death</i>	5±4	26±11	<b>29</b>	<b>55</b>
<i>Cell Survival</i>	95	74	71	
<i>p = 0.019</i>				
<b>RPMI-8226</b>				
<i>Cell Death</i>	3±2	6±2	<b>9</b>	<b>15</b>
<i>Cell Survival</i>	97	94	91	
<i>p = 0.011</i>				
<b>U266</b>				
<i>Cell Death</i>	4±2	2±1	<b>6</b>	<b>19</b>
<i>Cell Survival</i>	96	98	94	
<i>p = 0.019</i>				

## Figures

Figure 1

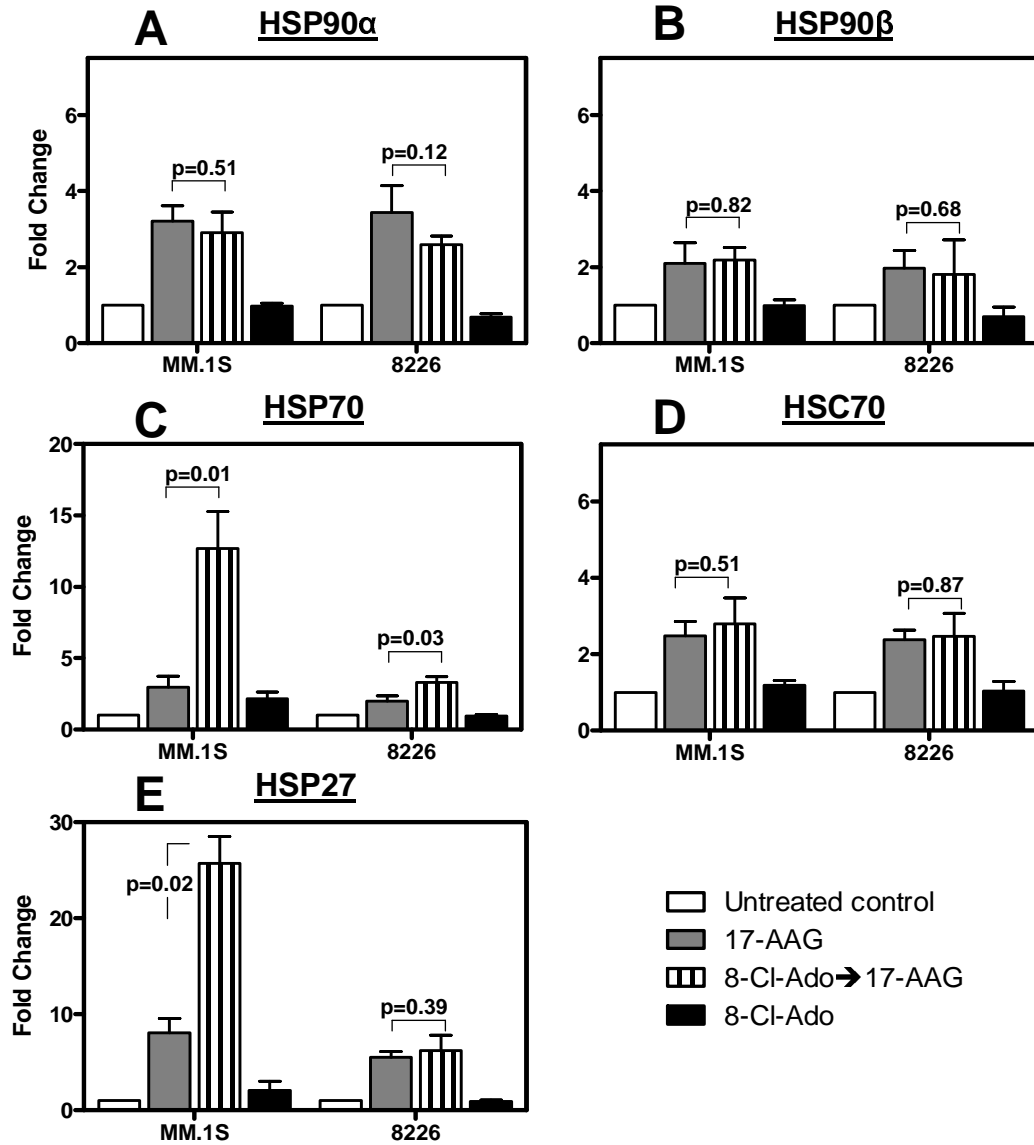






Figure 3

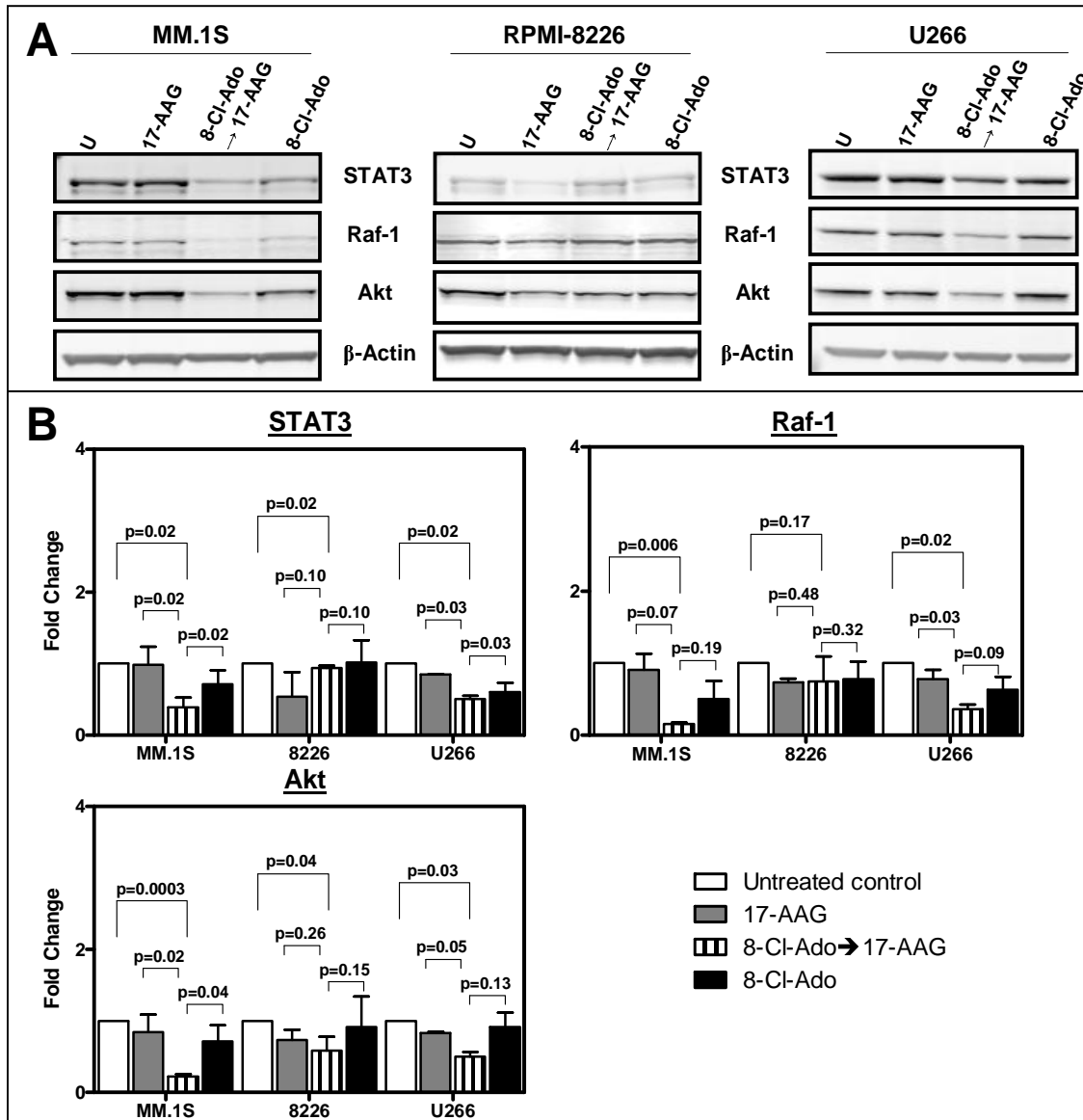


Figure 4

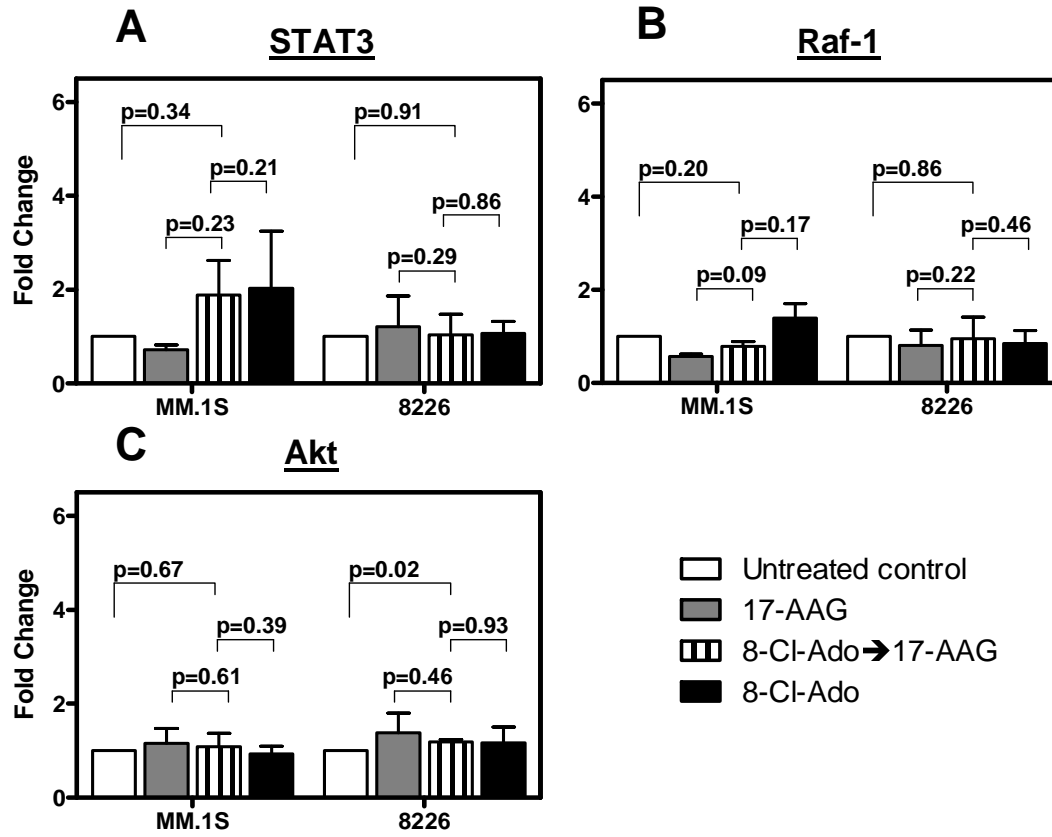


Figure 5

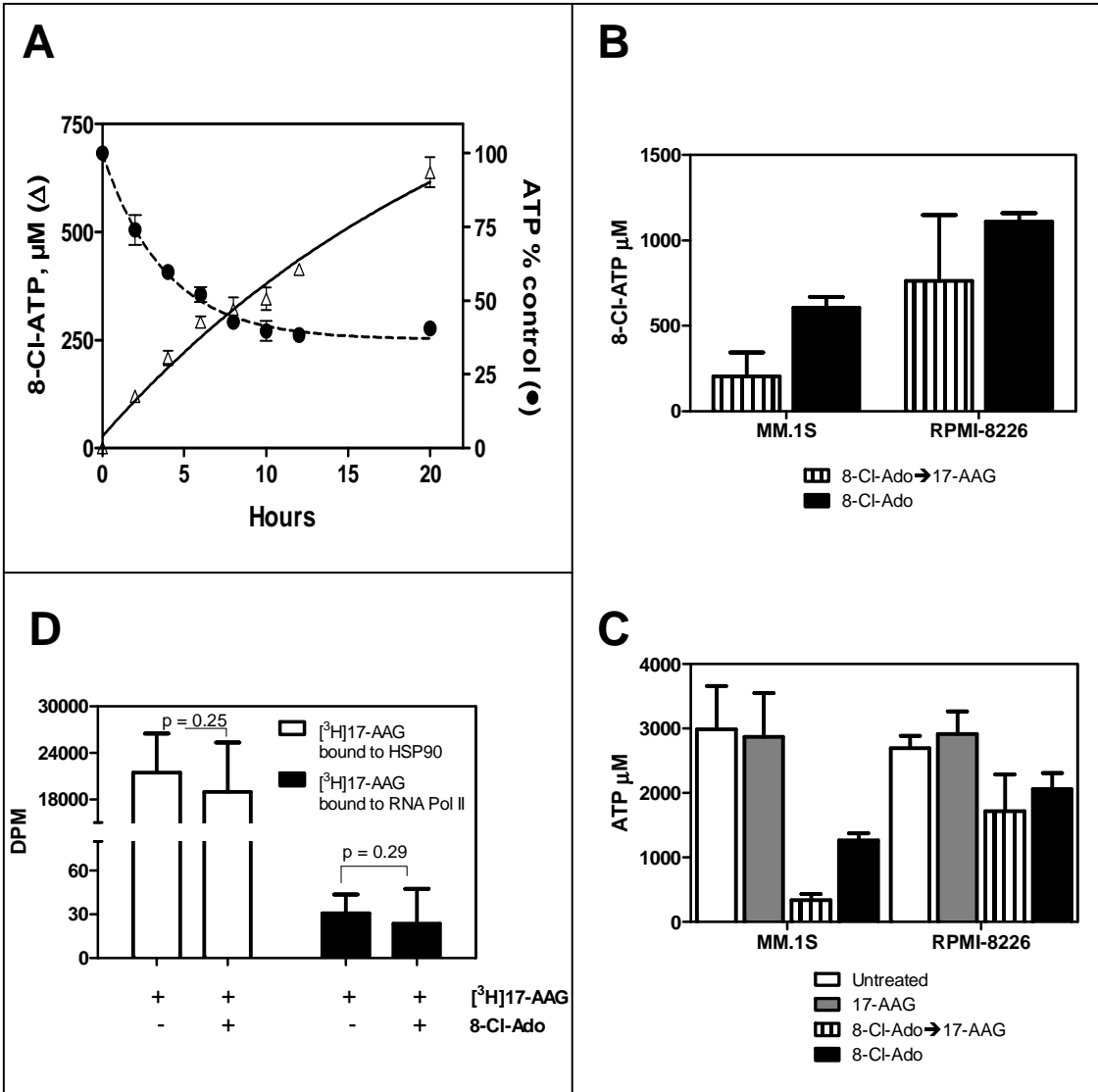


Figure 6

